www.czasopisma.pan.pl PAN POLSKA AKADEMIA NAUK www.journals.pan.pl

Arch. Metall. Mater., Vol. 61 (2016), No 4, p. 1739–1746

DOI: 10.1515/amm-2016-0279

M. LEŚNIAK*,#, J. PARTYKA**, M. SITARZ*

INFLUENCE OF SiO_2/Al_2O_3 MOLAR RATIO ON PHASE COMPOSITION AND SURFACES QUALITY OF ALUMINUM SILICATE SANITARY GLAZES IN THE SiO_2-Al_2O_3-CaO-Na_2O SYSTEM

This paper presents the results of research on aluminum silicate sanitary glazes in the SiO_2-Al_2O_3-CaO-Na_2O system with different SiO_2/Al_2O_3 molar ratio. XRD, SEM-EDS and FITR measurement indicated that SiO_2/Al_2O_3 molar ratio has a significant impact on the phase composition of the obtained glazes. Glass-ceramic glazes were obtained that consisted of both the glass phase and pseudowollastonite ($Ca_3[SiO_3]_3$) or anorthite ($Ca[Al_2Si_2O_8]$) crystals. Subsequently, the influence of phase composition on surface quality (roughness) was examined for the obtained samples. On the basis of the conducted examination of glaze surface roughness was observed that glazes of extreme SiO_2/Al_2O_3 molar ratio are characterized with greatest surface roughness when compared to other glazes.

Keywords: Glazes, SiO_2/Al_2O_3 molar ratio, microstructure, surface, roughness.

1. Introduction

Aesthetic and physical qualities of sanitary ceramic products are obtained by applying a glaze coating. In the structure of sanitary glazes in addition to the dominant glassy phase, which is a matrix coating are also crystalline phases [1]. The appearance of crystal phases results in non-transparent ceramic coatings on sanitary products (matte, muddy glazes). The type, amount and size of the crystals depend chiefly upon the chemical composition and firing conditions [2]. Inducing a controlled crystallization in glazes is achieved for example by decreasing the content of SiO_2, increasing the content of Al_2O_3 or as a result of increasing the proportion of alkaline earth metal oxides (CaO, MgO) in order to induce crystallization of silicates or aluminum silicates of these elements [3]. Crystal phases most frequently occurring in sanitary glazes include: wollastonite, pseudowollastonite, diopsyde, anorthite, albite, quartz, corundum, wilemite and zirconium silicate [4-7]. Wollastonite crystals ($CaSiO_3$) can occur in glazes in two polymorphic variations. The first variation is a triclinic form of calcium silicate of a chain construction. It forms elongated columnar crystals that are created as a result of a reaction of the product of limestone decomposition at approximately 600ºC ($CaCO_{3(s)} \rightarrow CaO(s) + CO_{2(g)}$) with silicon dioxide ($CaO_{(s)} + SiO_{2(s)} \rightarrow CaO \cdot SiO_{2(s)}$) [8]. Wollastonite may also occur in high-temperature variation also known as psedudowollastonite. Polymorphic transformation of β form into α form is an irreversible process that takes place at 1125±10ºC and is accompanied by a slight increase in the crystals volume. Pseudowollastonite belongs to the group of ring silicates and its 12th chain consists of Si_3O_9 units. This form builds hexagonal crystals and usually occurs in glazes when MgO/CaO molar ratio is higher than 0.01 [9-11]. Roughness of the glaze surface depends on the course of the glaze melting during the firing process (heat processing). A proper spreading of the glaze on the ceramic surface depends on its viscosity and surface tension. The effects of surface tension are visible in the tendency to cover the least surface area possible and constitute a significant factor influencing the glaze's ability to eliminate the roughness and smooth the surface [12]. The quality of a glazed product is also affected by the amount and type of crystal phases contained in the glassy matrix. When crystals reach above a glassy matrix the microroughness of the coating increases. The effect is undesirable, because light falls on a rough surface and diffused reflection occurs. Thus, the required optical properties (gloss, color) of glaze are deteriorated. An increase in roughness has a substantial impact also on the lowering of chemical resistance against water and strongly alkaline cleaners and disinfectants. The majority of surface flaws, including roughness occur in the areas of extensive energy - in such areas, chemical corrosion starts. Additionally, excessive roughness is conducive to the deposition of dirt (mainly sediments) on the glaze surface [13,14].

2. Experimental procedure

2.1. Preparation of research materials

The subject of this paper is the research of aluminumsilicate glazes in a multicomponent system of the SiO_2-Al_2O_3-CaO-

* AGH UNIVERSITY OF SCIENCE AND TECHNOLOGY, FACULTY OF MATERIALS SCIENCE AND CERAMICS, DEPARTMENT OF SILICATE CHEMISTRY AND MACROMOLECULAR COMPOUNDS, AL. A.MICKIEWICZ 30, 30-059 KRAKÓW, POLAND

** AGH UNIVERSITY OF SCIENCE AND TECHNOLOGY, FACULTY OF MATERIALS SCIENCE AND CERAMICS, DEPARTMENT OF CERAMICS AND REFRACTORY MATERIALS, AL. A.MICKIEWICZ 30, 30-059 KRAKÓW, POLAND

Corresponding author: mlesniak@agh.edu.pl

Na_2O at a firing temperature of 1220-1250ºC by variable molar retio of SiO_2/Al_2O_3. Samples were marked as: Ca1Na–Ca6Na. The following substances were used as introducers for particular oxides: quartz flour (manufacturer: SKSM Sobótka, Poland), aluminum oxide (manufacturer: Helmut Kreutz GmbH), sodium carbonate (Na_2CO_3) (manufacturer: Avantor Poland) and chalk (manufacturer: ZPSChiM "PIOTROWICE" Sp. z o.o. Poland). Preparation of samples started with weighing all components in accordance with the formula. Sets of materials were ground in a planetary grinder for 30 minutes until 0.1% residue on a 0.063 mm strainer. Dried, raw glazes were placed in porcelain crucibles of an approximate volume of 90 cm^3 and then simultaneously fired in an electric laboratory oven at 1230ºC for 14 hours. Glazes thus obtained were used to prepare samples for further examinations. Samples for the scanning electron microscope (SEM) were cut into 4mm x 15mm x 15mm cuboids. One of the large surfaces was additionally polished. The remaining material (fired glazes) was crumbled into grains smaller than 0.063 mm. The powders were used to mark the chemical composition and phase composition. In order to obtain information on the chemical composition of the fired glazes, wavelength dispersive X-ray fluorescence (WDXRF) analysis was applied. The analysis of the chemical composition was performed with a WDXRF Axios mAX Spectrometer produced by PANalytical. Phase composition of the fired experimental glazes was marked using X-ray diffraction conducted with an X'Pert Pro X-ray diffractometer produced by PANalytical. Diffractometers had a measuring scope of 5–90º (2Θ) and a measuring speed of 0.05º 2Θ/2s. Additional information on the phase composition of the glazes was provided by middle-infrared spectroscopy (MIR). FTIR examination was performed with a Bruker Optics-Vertex70V Fourier spectrometer. The samples were prepared as KBr pellets. Absorption spectra were registered with 128 scans and a resolution of 4 cm-1. Microstructure of the glazes was examined as well. The observations were conducted for micro sections using a SEM-FEI Nova 200 scanning electron microscope NanoSEM with an element composition analyzer in micro areas (SEM-EDS). Examination of surface roughness was conducted with OLYMPUS LEXT 4000 laser confocal microscope using the 20x magnification. The scanned area of the examined samples covered approximately 4.68 mm^2.

3. Results

3.1. Chemical composition of glazes

An analysis of the chemical composition of the examined glazes after firing is presented in TABLE 1. On the basis of the obtained data it was observed that, as planned, the content of SiO_2 decreases in consecutive samples, while the content of A_2O_3 increases. The main establishment of the research – lowering the SiO_2/Al_2O_3 molar ratio - was thus completed. As for modifying oxides, CaO and Na_2O, a standard diffraction of their content in particular glazes did not exceed ±2%.

TABLE 1

Oxide composition of experimental glazes after firing

Glaze	SiO_2	Al_2O_3	CaO	Na_2O
	wt [%]			
Ca1Na	70.39	7.17	14.03	7.68
Ca2Na	67.70	9.63	13.99	7.97
Ca3Na	65.49	12.02	14.36	7.65
Ca4Na	63.07	14.57	14.14	7.81
Ca5Na	60.32	16.63	14.53	8.07
Ca6Na	55.93	19.07	15.58	9.05

3.2. Phase composition of glazes

The tests of the phase composition (XRD) of fired glazes (Fig.1) showed that all experimental glazes were composite materials. Apart from amorphous phase (raised background in the scope: 2θ: 10-30º) a number of reflections occurs confirming the presence of crystal phases. The conducted analysis led to the conclusion that Ca1Na-Ca4Na glazes contain a calcium silicate pseudowollastonite of the ring silicates group ($Ca_3[SiO_3]_3$), while Ca5Na and Ca6Na glazes contain calcium aluminum silicate – anorthite of aluminum tectosilicates group ($Ca[Al_2Si_2O_8]$) [15,16].

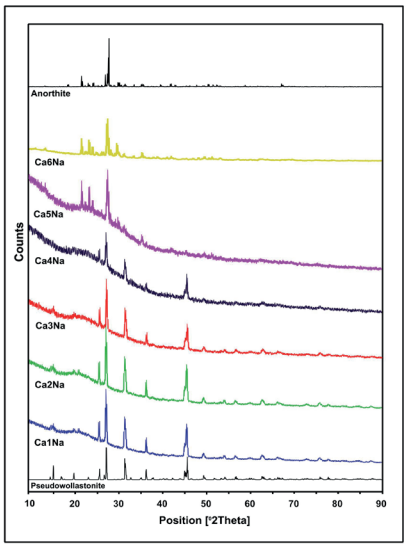

Fig.1. Diffractograms of fired glazes

3.3. Scanning electron microscopy (SEM-EDS)

Scanning electron microscopy (SEM-EDS) allowed one to assess the microstructure of the examined samples, mainly the size and shape of crystallites (Fig.2-7). Analysis of the SEM images confirmed the results of the phase analysis: all the examined glazes were glass-ceramic materials. The presented images (Fig.2-7) demonstrate, apart from the amorphous phase, a distinct image of crystals of various sizes and habits. The performed analysis of the chemical composition in micro areas (SEM-EDS) indicated that in the case of Ca1Na-Ca4Na glazes, the visible crystals were virtually pure calcium silicate,

whereas in the case of Ca5Na and Ca6Na glazes, calcium aluminum silicate was observed (Fig.2-7). Considering the intensity ratios of particular peaks in the EDS spectra, it might be observed that the visible crystals were, respectively, pseudowollastonite (glazes Ca1Na-Ca4Na) and anorthite (glaze Ca5Na and Ca6Na).

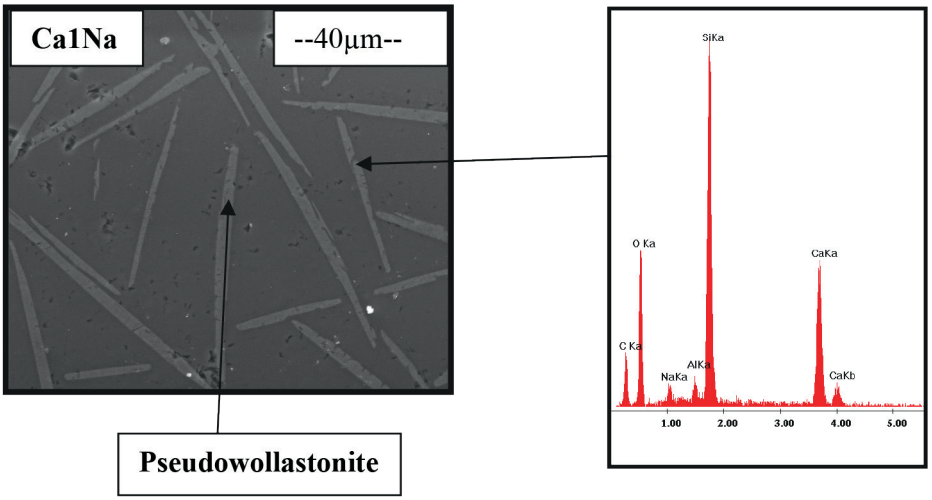

Fig. 2. SEM image of Ca1Na glaze with chemical composition analysis of crystal phase

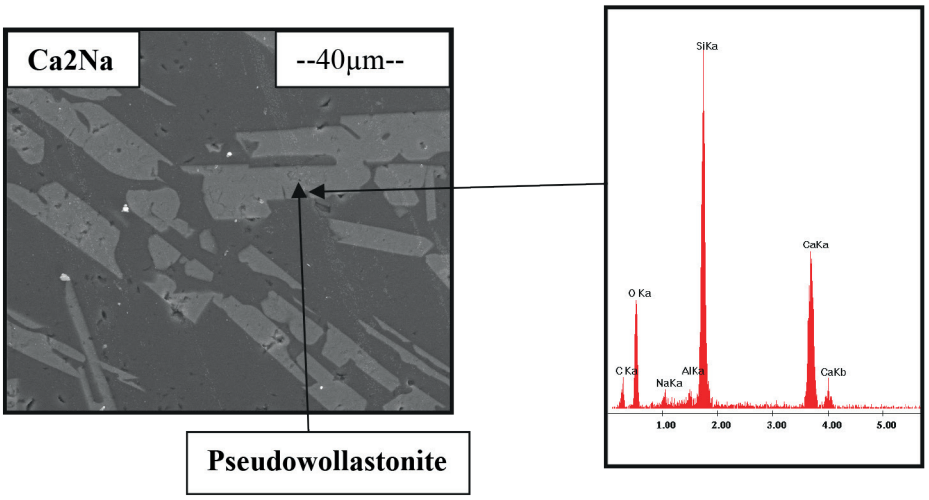

Fig. 3. SEM image of Ca2Na glaze with chemical composition analysis of crystal phase

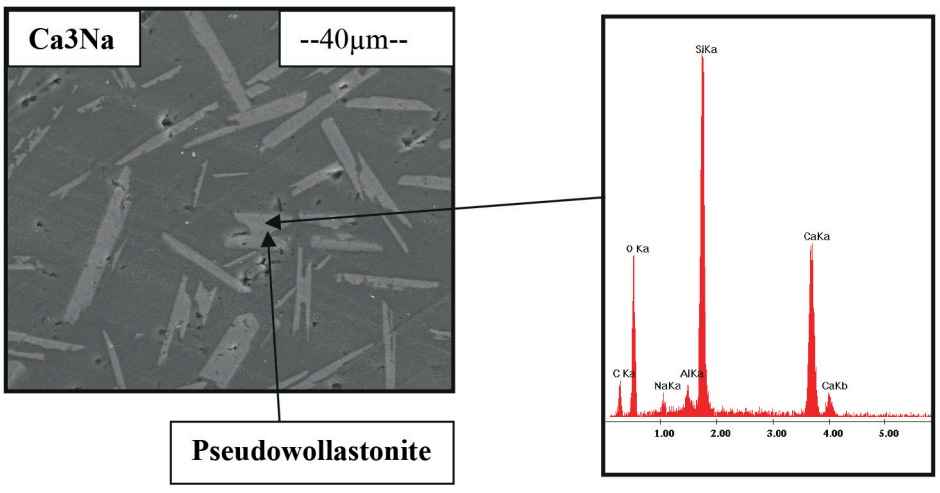

Fig. 4. SEM image of Ca3Na glaze with chemical composition analysis of crystal phase

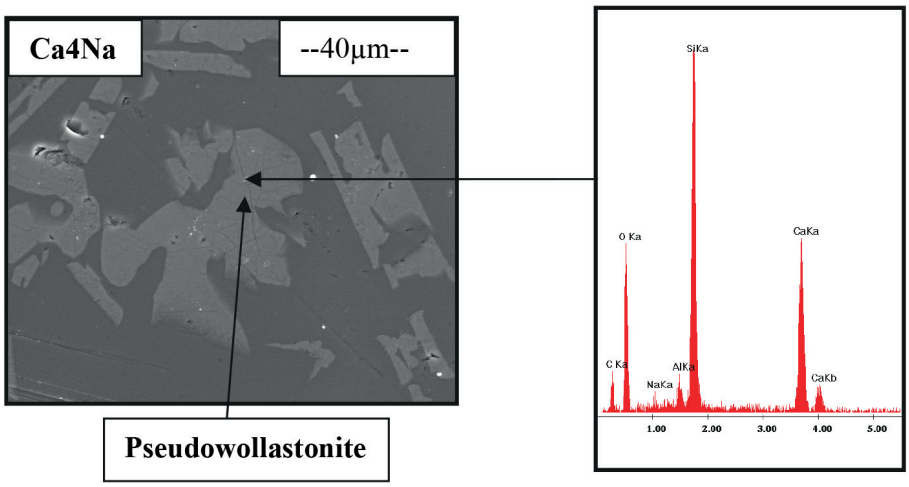

Fig. 5. SEM image of Ca4Na glaze with chemical composition analysis of crystal phase

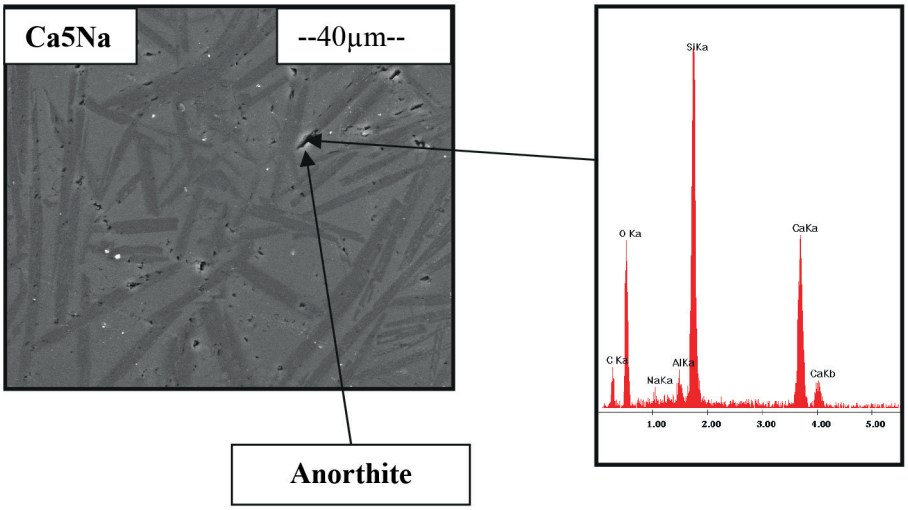

Fig. 6. SEM image of Ca5Na glaze with chemical composition analysis of crystal phase

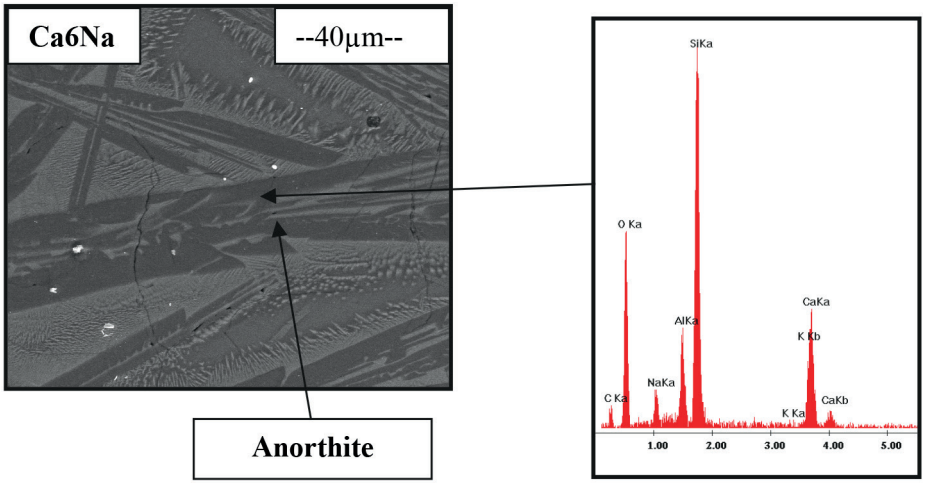

Fig. 7. SEM image of Ca6Na glaze with chemical composition analysis of crystal phase

By examining the SEM images, it may be observed that the decrease of SiO_2/Al_2O_3 content molar ratio is accompanied by alterations of crystals' habit. With a high content of silicone dioxide and a low content of aluminum oxide, pseudowollastonite crystals form in the shape of elongated crystal needles. As the SiO_2/Al_2O_3 content ratio decreases, crystals form into columns and then into amorphous, elongated facet plates. Anorthite crystals' habit changes as well: from column crystals to irregular facet plates and non-faceted plates.

3.4. Spectroscopic studies

Sanitary ceramic glazes designed for firing temperatures higher than 1200ºC are most frequently aluminumsilicate materials. MIR spectra of aluminumsilicate materials in 1400-400 cm^{-1} show ranges related to vibrations of silicon-oxygen bonds and aluminum-oxygen bonds. Fig.8 demonstrates MIR spectra of all examined glazes and Fig.9, Fig.10 present a comparison of the spectra and model spectrum of phases registered after XRD and SEM-EDS examinations: respectively of pseudowollastonite (Fig.9) and anorthite (Fig.10). All spectra presented in Fig.8 are characterized by the presence of three groups of ranges located at 1350-900 cm^{-1}, 850-650 cm^{-1} and 500-400 cm^{-1}. The high full width at half maximum confirms the high proportion of amorphous phase in the examined glazes.

It was proved through XRD and SEM-SEM examinations that the crystal phases present in Ca1Na-Ca4Na glazes are pseudowollastonite. MIR spectra of each three-membered ring silicate contain a specific intense range at 750-700 cm^{-1}, due to its presence in the structure of isolated 3-membered silicon-oxygen rings. Easily noticeable in MIR spectra of Ca1Na-Ca4Na glazes (Fig.9) is a range at approximately 716 cm^{-1}, which clearly confirms the presence of pseudowollastonite

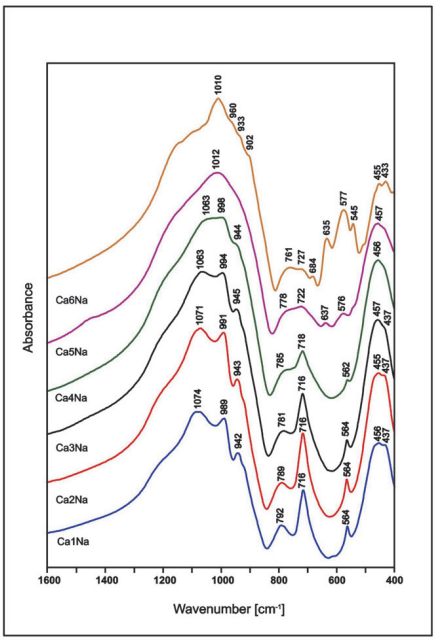

Fig. 8. MIR spectra of the glazes

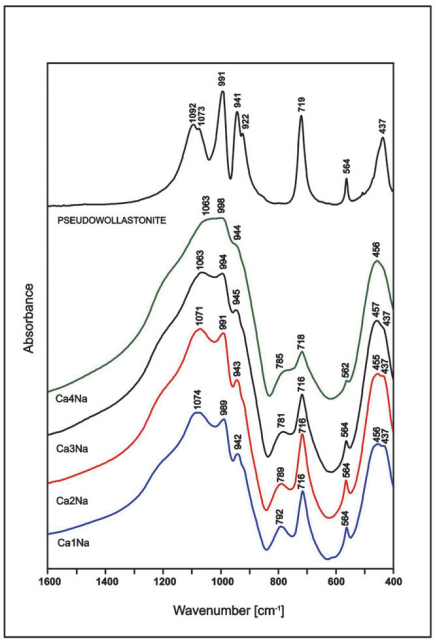

Fig. 9. MIR spectra of Ca1Na-Ca4Na glazes and spectrum of pseudowollastonite [15]

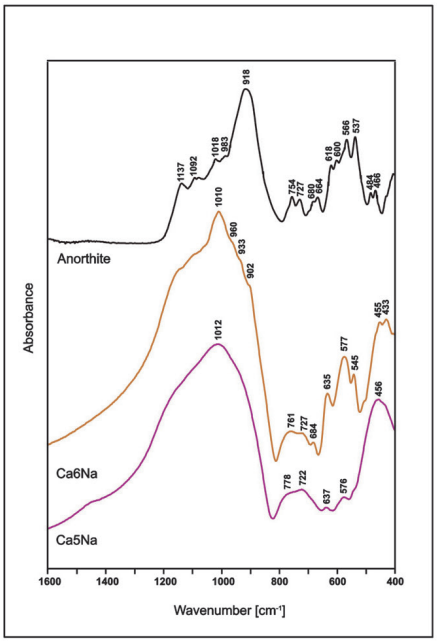

Fig. 10. MIR spectra of Ca5Na-Ca6Na glazes and spectrum of anorthite [16]

[17]. Moreover, by comparing spectra of the experimental glazes (Ca1Na-Ca4Na) with MIR spectrum of pure pseudowollastonite (Fig.9), ranges can clearly be ascribed to pseudowollastonite at approximately 991 cm^{-1} (stretching vibrations of Si-O(Si)), 945 cm^{-1} (stretching vibrations of $Si-O^-$) and 562 cm^{-1} (bending vibrations of Si-O-Si). Other ranges are related chiefly to the remaining amorphous phase. By comparing MIR spectrum of Ca6Na glaze with MIR spectrum of anorthite (Fig.10), it can be assumed that the group of ranges at 630-540 cm^{-1} (bending vibrations of Si-O-Si and Si-O-Al) is related to anorthite in the MIR spectrum of Ca6Na glaze [18-20]. By comparing MIR spectrum of Ca5Na glaze with MIR spectrum of Ca6Na, a distinct difference can be observed in terms of the degree of crystallized anorthite. Hence, the identification of ranges characteristic of anorthite in the spectrum of Ca5Na is considerably more difficult. Moreover, anorthite is an aluminum tectosilicate, and therefore ranges related to vibrations of silicon-oxygen bonds and aluminum-oxygen bonds are equal as vibrations of such bonds in the amorphous phase.

3.5. Examination of surface roughness

On the basing of the R_a parameter obtained for each of the glazes average values were calculated along with confidence intervals. Results of the calculations are presented in TABLE 2. The Ra parameter was calculated from 10 linear measurements conducted on a sample surface: 2 perpendicular sets, each of 5 measurements. An image of linear profiles of each glaze is presented in Figure 11.

The most uneven surface among all examined glazes was observed with Ca6Na glaze (Ra=0.519) and Ca1Na glaze (Ra=0.462). The highest value of Ra parameter for these glazes is undoubtedly related to the presence of crystal phases in the glassy matrix that increases glaze surface roughness. It should also be observed that Ca1Na and Ca6Na are glazes of extreme SiO_2/Al_2O_3 molar ratio (Table 1). This can be explained with the fact that both Al_2O_3 and SiO_2 are oxides characterized by high melting temperatures. During the heat processing of glazes, it is particularly important that the first portion of the liquid phase appears at low temperatures, as it enables a larger amount of material grains to melt and thus results in a smoother surface. The smoothest surface of all samples was obtained for the Ca4Na glaze. On the basis of the XRD examination the presence of pseudowollastonite crystals and amorphous phase in this glaze was confirmed. When analyzing the values of the Ra parameter for Ca1Na-Ca4Na glazes, a tendency can be observed of the value increase proportionate to the increase of silicon dioxide (SiO_2) in the composition of these glazes. The surface of each glaze measured during the roughness examination is presented in Figures 12 – 17. Two-dimensional (2D) and three-dimensional (3D) images were prepared.

TABLE 2

Average Ra values and confidence intervals for glazes that underwent the examination of surface roughness

Glaze	Ca1Na	Ca2Na	Ca3Na	Ca4Na	Ca5Na	Ca6Na
R_a [µm]	0.462	0.475	0.301	0.217	0.335	0.519
σ	±0.095	±0.078	±0.404	±0.030	±0.072	±0.156
Min	0.358	0.368	0.134	0.178	0.233	0.296
Max	0.618	0.605	0.649	0.265	0.462	0.777

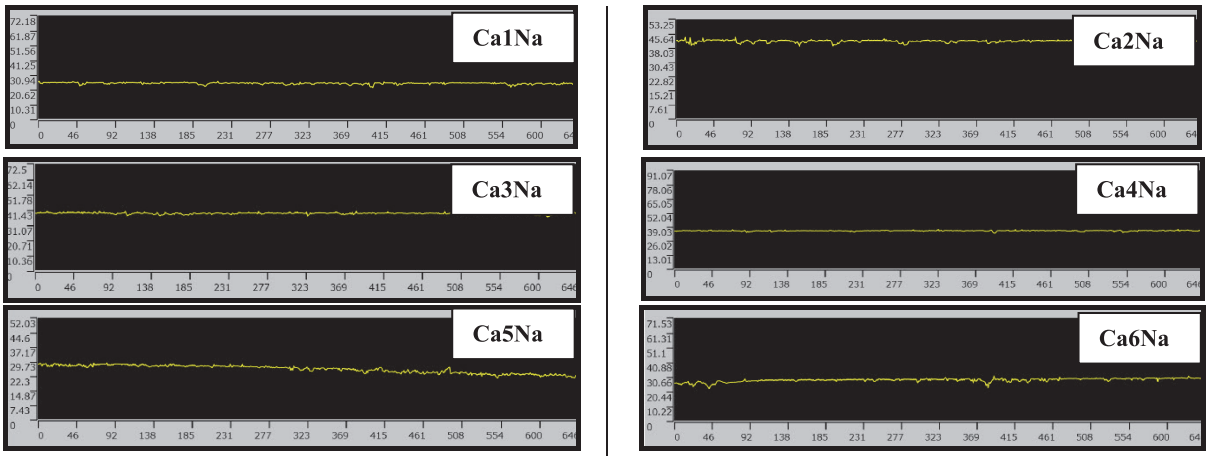

Fig. 11. Linear profile of all glazes at 20x magnification

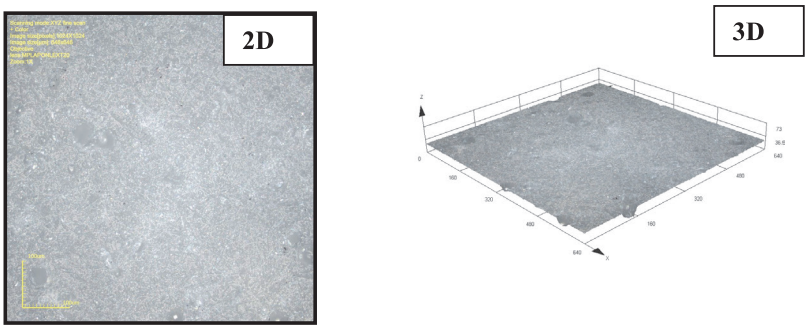

Fig. 12. Two- and three-dimensional images of Ca1Na glaze surface

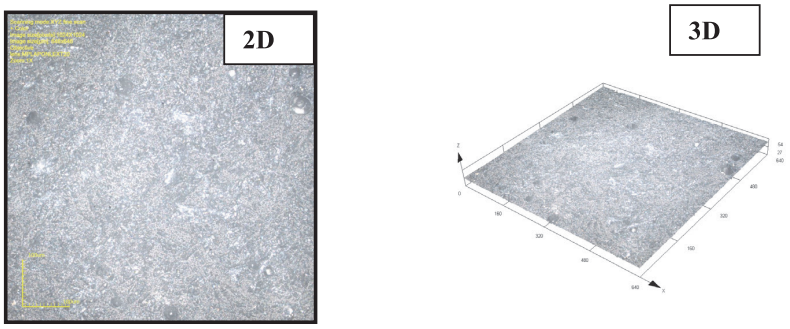

Fig. 13. Two- and three-dimensional images of Ca2Na glaze surface

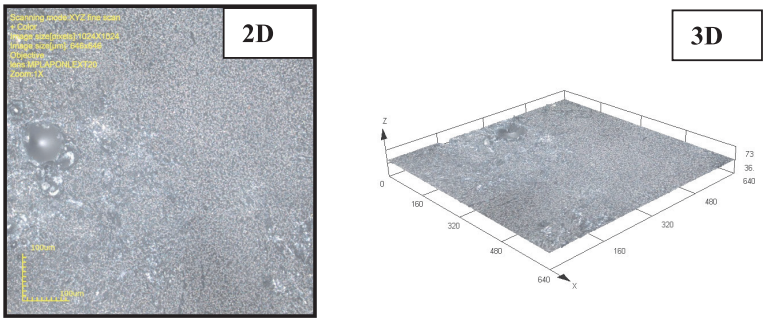

Fig. 14. Two- and three-dimensional images of Ca3Na glaze surface

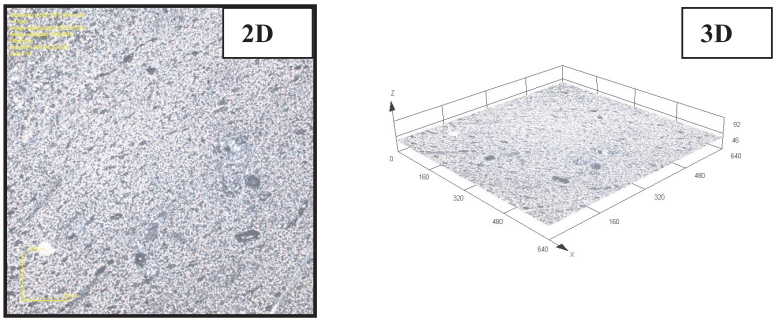

Fig. 15. Two- and three-dimensional images of Ca4Na glaze surface

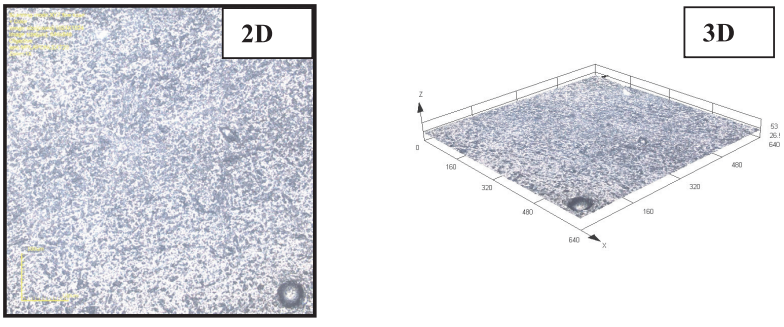

Fig. 16. Two- and three-dimensional images of Ca5Na glaze surface

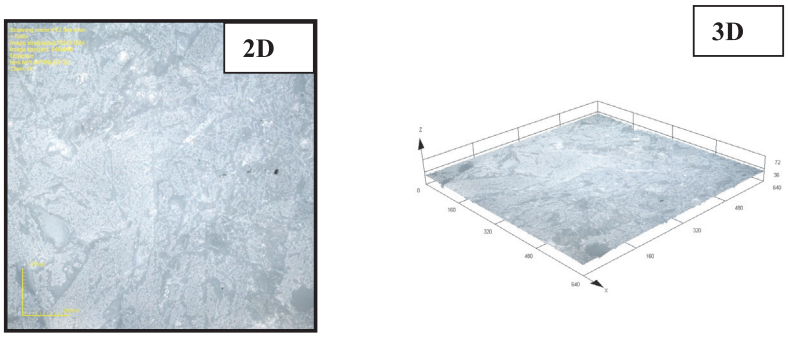

Fig. 17. Two- and three-dimensional images of Ca6Na glaze surface

4. Conclusions

- Changing of the SiO_2/Al_2O_3 molar ratio in the SiO_2-Al_2O_3-CaO-Na_2O system has a decisive influence on the type and amount of the crystalline phase in the obtained glazes.
- At the highest SiO_2/Al_2O_3 moar ratio the examined glazes are glass-ceramic composites that, apart from the glass phase contain calcium silicate pseudowollastonite.
- At the SiO_2/Al_2O_3 molar ratio equals 3.23 the material contains a glass phase and calcium aluminum silicate - anorthite.
- Changing of the SiO_2/Al_2O_3 molar ratio significantly affects the size and habit of crystal grains of both types: pseudowollastonite and anorthite.
- The presence of the crystal phase in the presented glass-ceramic glazes has a considerable impact on the quality (roughness) of their surface.
- Glazes of extremely different content of SiO_2 and Al_2O_3 are characterized with the highest value of the Ra parameter when compared to other glazes.

Acknowledgments

This work was carried out thanks to support from NCBiR grant number PBS1/B5/17/2012.

REFERENCES

[1] J. Partyka , J. Lis, Ceram. Intern. **37**, 1285-1292 (2011).
[2] V.I. Voevodin, Glass and Ceramics. **57**, 250-251 (2000).
[3] J.Ma. Rincón, M. Romero, J. Marco, V.Caballer, Mate. Res. Bull. **33**, 1159-1164 (1998).
[4] K.S. Kutateladze, G.G. Gaprindashvili, G.Z. Loladze, O.A. Gladushko, Glass and Ceramics **37**, 357-358 (1980).
[5] O.S. Grum-Grzhimailo, K.K. Kvyatkovskaya, L.M. Savvateeva, Glass and Ceramics **35**, 41-43 (1978).
[6] L. Fröberg, L. Hupa, M. Hupa, J. Eur. Ceram Soc. **29** ,7-14 (2009).
[7] T. Kronberg, L. Hupa, K. Fröberg, Adv. Sci. Technol. **45**, 590-595 (2006).
[8] L. Fröberg, Åbo Akademi, 2007 Åbo.
[9] P. Richet, B.O. Mysen, J. Ingrin, Phys. Chem. Miner. **25**, 401-414 (1998).
[10] J. Jeffery, W. Heller, L. Preliminary, Acta Cryst. **6**, 807-808 (1953).
[11] T. Yamanaka, H. Mori, Acta Cryst. **B37**, 1010-1017 (1981).
[12] J.F. Mejia, Understanding the role of fluxes in single-fire porcelain glaze development, 2004 Alfred University, New York.
[13] T. Kronberg, A. C. Ritschkoff, R. Mahlberg, J. Mannila, M. Kallio, A. Vesa, L. Hupa. J. Eur. Ceram Soc. **27**, 1775–1780 (2007).
[14] W.B. White, Theory of corrosion of glass and ceramics: Corrosion of glass, ceramics and ceramic superconductors: principles, testing, characterization, and applications, 1992 Park Ridge: Noyes Publications, 2–28.
[15] http://rruff.info/pseudowollastonite/display=default/R070762
[16] http://rruff.info/anorthite/display=default/R040059.
[17] M. Sitarz, M. Handke, W. Mozgawa, E. Galuskin, I.O. Galuskina, J. Mol. Struct. **555**, 357-362 (2000).
[18] M. Sitarz, J. Non-Cryst. Sol. **357**, 1603-1608 (2011).
[19] W. Mozgawa, M. Sitarz, M. Rokita, J. Mol. Struct. **511**,-512, 251-257 (1999).
[20] W. Mozgawa, M. Sitarz, J. Mol. Struct. **614**, 273-279 (2002).